Entropy **2015**, *17*, 2355-2366; doi:10.3390/e17042355

OPEN ACCESS

entropy

ISSN 1099-4300

www.mdpi.com/journal/entropy

Article

A Criterion for Topological Close-Packed Phase Formation in High Entropy Alloys

Yiping Lu [1,2,†] Yong Dong [1,†], Li Jiang [1], Tongmin Wang [1,*], Tingju Li [1,3] and Yong Zhang [4,*]

[1] School of Materials Science and Engineering, Dalian University of Technology, Dalian 116024, China; E-Mails: luyiping@dlut.edu.cn (Y.L.); dongyong5205@mail.dlut.edu.cn (Y.D.); jiangli@mail.dlut.edu.cn (L.J.); tjuli@dlut.edu.cn (T.L.)

[2] State Key Laboratory of Metastable Materials Science and Technology, Yanshan University, Qinhuangdao 066004, China

[3] Key Laboratory of Materials Modification by Laser, Ion, and Electron Beams, Ministry of Education, Dalian University of Technology, Dalian 116024, China

[4] State Key Laboratory for Advanced Metals and Materials, University of Science and Technology Beijing, Beijing 100083, China

† These authors contributed equally to this work.

* Author to whom correspondence should be addressed; E-Mail: tmwang@dlut.edu.cn (T.W.); drzhangy@ustb.edu.cn (Y.Z.); Tel.: +86-411-84709400 (T.W.).

Academic Editor: Kevin H. Knuth

Received: 19 January 2015 / Accepted: 15 April 2015 / Published: 20 April 2015

Abstract: The stability of topological close-packed (TCP) phases were found to be well related to the average value of the d-orbital energy level ($\overline{Md}$) for most reported high entropy alloys (HEAs). Excluding some HEAs that contain high levels of the elements aluminum and vanadium, the results of this study indicated that the TCP phases form at $\overline{Md} > 1.09$. This criterion, as a semi-empirical method, can play a key role in designing and preparing HEAs with high amounts of transitional elements.

Keywords: high entropy alloys; TCP phases; d-orbital energy level; alloy design

---

1. Introduction

New types of alloy, which include high entropy alloys (HEAs) and multi-component alloys with equiatomic and near-equiatomic compositions, are garnering much research attention in the metallic materials community [1–3]. Compared to conventional metallic alloys based on one or two major elements, these new alloys generally contains 5–13 principal elements [2]. These alloys were named multi-component alloys by Cantor *et al.* [1] and defined as HEAs by Yeh *et al.* [2]. To date, many promising properties have been reported, including highly wear-resistant HEAs like $Co_{1.5}CrFeNi_{1.5}Ti$ and $Al_{0.2}Co_{1.5}CrFeNi_{1.5}Ti$ [4,5]; high-strength body-centered-cubic (BCC) structured $AlCoCrFeNiTi_{0.5}$ and $AlCrFeNiMo_{0.2}$ HEAs (at room temperature) [6,7], and NbMoTaV HEA (at elevated temperatures) [8,9], and high corrosion resistant $Cu_{0.5}NiAlCoCrFeSi$ HEA [10]. Researchers are drawn to HEAs due to their unique compositions, microstructures, and adjustable properties. To date, many studies have been performed on HEAs, and they have become a hot topic for research in the materials community [11–32].

HEAs generally consist of simple solid solutions of face centered cubic (FCC) structures, body centered cubic (BCC) structurs or a combination of the two. Research findings show that a small quantity of intermetallic compound phase/metastable particles often form in HEAs after solidification or the completion of an aging treatment at intermediate temperatures [3,25,33]. These intermetallic compound phases/metastable particles, especially the topological close-packed (TCP) phases, are closely related to the mechanical properties of HEAs. Therefore, it is necessary to predict the occurrence of TCP phases which include the Laves phase, σ phase, R phase, μ phase, P phase, and so on.

In the past, most HEAs contained the elements Co, Fe, and Ni as their primary elements. Usually, some alloying elements, such as Al, B, Cr, Mo, Nb, Si, Ti, V, are added to HEAs that contain Co, Fe and Ni, forming alloy systems such as $Al_{0.5}CoCrCuFeNiTi_x$ [34], $Al_{0.5}CoCrCuFeNiB_x$ [35], $Al_{0.5}CoCrCuFeNiV_x$ [36], $AlCoCrFeNiMo_x$ [37], $AlCoCrCuFeNiMo_x$ [38], $AlCoCrFeNiTi_x$ [6], $AlCoCrFeNiNb_x$ [39], $AlCoCrFeNiSi_x$ [40], and $AlCoCrFeNiTi_{0.5}$ [41]. It is worth noting that when the concentrations of Al, B, Cr, Mo, Nb, Si, Ti, and V exceed a critical value, some ordered phases might form, which could deteriorate the plasticity of the HEAs. For example, the plastic strain of as-cast $AlCoCrFeNiNb_{0.25}$ alloy is remarkably lower than that of as-cast AlCoCrFeNi alloy due to the formation of the Laves phase [39]. Taking $AlCoCrFeNiNb_x$ alloys [39] as an example again, with the increase of x, the crystal structure of the alloys can transform from BCC to BCC + Laves phase. Although both the yield strength and hardness increase, the plasticity decreases dramatically. Another case to illustrate this point includes the structural transformation sequence for the $CoCrFeNiMo_x$ system, where with the increase of x, it has been observed that FCC → FCC + σ → FCC + σ + μ [42]. The formation of the σ phase is considered to be due to two factors, one of which is the identical crystal structure and the similar electron configuration between Cr and Mo, and the other is the substitution capability among Co, Fe, and Ni elements. Similarly, in $AlCoCrFeNiNb_x$ and $CoCrFeNiTi_x$ HEAs, the TCP phase forms with an increased content of Nb and Ti elements, which is explained by the large atomic size of Nb and Ti elements as well as its large negative enthalpies of mixing with other alloying elements [6,43]. However, the experimental results are far from proving this satisfactorily.

Recently, the valence electron concentration (VEC) was used to predict the existence of the σ phase, a TCP phase, in Cr- and/or V-containing HEAs [33] where the criterion worked well. Electronegativity was also successfully used to predict TCP phases in HEAs [44]. Yang *et al.* successfully used a simple

thermodynamic rule, *i.e.*, the entropic and the average heat of mixing, to predict phase selection in multicomponent alloys [45]. Liu *et al*. proposed an effective atomic size parameter to predict the phase stability in multicomponent systems [46]. These semi-empirical modes have achieved great success in predicting the stability of solid solution phases of HEAs. The d-orbital energy level (*Md*) physically correlates with electronegativity and metallic radius of elements, both of which are parameters used in the classical approach by Hume-Rothery and Darken and Gurry [47]. For example, the *Md* value will increase with the increase of metallic radius, and it will reduce with the increase of electronegativity, so the parameter *Md* has great potential for dealing with the stability of TCP, especially in those HEAs containing high mounts of certain transitional elements. Therefore, in this paper, another parameter was used: the average value of the energy level of d-orbital ($\overline{Md}$) parameters to predict all types of TCP phases of HEAs.

2. Results and Discussion

It is generally accepted that d-electron bonding is of great significance to the metallurgical properties of transition metals. The average value of the d-orbital energy level was proposed as:

$$\overline{Md} = \sum_{i=1}^{n} C_i (Md)_i$$

where C_i is the atomic fraction of component *i* in the alloy, and $(Md)_i$ is the d-orbital energy level of element *i* in the *M*-element centered cluster in the *i*-*M* binary solid solution alloy, in which *i* is a solvent and *M* is a solute. This was proposed to design superalloys by Morinaga, *et al.* [47–51], who found that all of the Ni-based, Co-based, and Fe-based superalloys with the σ phase formed displayed higher $\overline{Md}$ values (about 0.915) than those of alloys without forming the σ phase. To data, the $\overline{Md}$ parameter has been successfully used to design superalloys. In HEAs, most principle elements are transition elements similar to superalloys. Therefore, in this paper, the parameters $\overline{Md}$ can be adopted to study the stability of the TCP phase in HEAs that contain more transitional elements.

In HEAs, the matrix and commonly added alloying elements, including Ni, Fe, Co, Cr, and so on, have FCC, BCC, or a combination of the two as a structure. Previous research shows that the $(Md)_i$ value of transition metals in the BCC-structured Fe is slightly higher than that of transition metals in the FCC-structured Ni_3Al, although they display the same variation trend [50,52]. It seems possible to establish a semi-empirical model to predict the presence of TCP phases in HEAs. When a new HEA is designed, the accurate structure was not known before testing, so in order to calculate its $\overline{Md}$ value, it was necessary to assume a single structure for HEAs. According to previous research results, whether adopting the FCC structure or BCC structure, the $(Md)_i$ value was almost the same. Therefore, the assumed single structure may be a FCC or BCC structure, regardless of the real structure the HEA. For calculation convenience, all HEAs in this study were assumed to have a single FCC Ni_3Al structure when the $\overline{Md}$ values were calculated. Thereunto, the $(Md)_i$ value was the individual element which was calculated based on the FCC Ni_3Al structure, which is shown in Figure 1a. An Al atom is surrounded by twelve Ni atoms as its nearest neighbours, and surrounded by six Al atoms in its second nearest neighbours. The cluster used in the calculation was $[MNi_{12}Al_6]$, which is shown in Figure 1b. An Al

atom in the center was substituted for the various alloying elements of M (M = Ti, Cr, Mn, Fe, Co, Ni, Cu, V, Mo, and so on). More details can be found in Refs. [47,48].

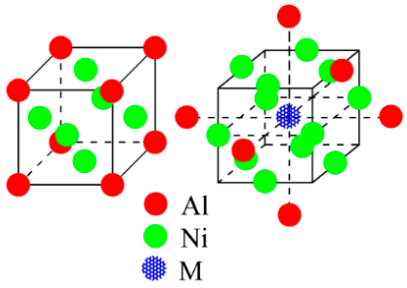

Figure 1. The calculation of $(Md)_i$ value: **(a)** Crystal structure of Ni_3Al; and **(b)** Cluster model used in the calculation.

Although the $(Md)_i$ values calculated in BCC/(BCC + FCC)-structured HEAs were slightly lower than the actual data, this approach could successfully predict the stability of the TCP phase by providing a reasonable guideline.

According to the methods reported by Morinaga [47–50], the value of the parameter $\overline{Md}$ was calculated for the reported HEA system that contained TCP phases. The values are shown in Table 1 [5,6,34,36–38,39,42,43,53–65]. It was found that all the HEAs in Table 1 were synthesized by arc melting and then solidified in a water-cooled copper hearth. As can be seen, a rule emerges in that TCP phases occurred when the value of $\overline{Md}$ reached 1.09.

Table 1. The crystal structure and the parameters, $\overline{Md}$, for typical reported multi-component HEAs.

Alloys	Structure	$\overline{Md}$ (eV)	Refs
$AlCoCrFe_{0.6}NiMo_{0.5}$	BCC + σ phase	1.1423	5
$AlCoCrFe_{1.0}NiMo_{0.5}$	BCC + σ phase	1.1216	5
$AlCoCrFe_{1.5}NiMo_{0.5}$	BCC + σ phase	1.0997	5
$AlCoCrFe_{2.0}NiMo_{0.5}$	BCC + σ phase	1.0811	5
$AlCo_{0.5}CrFeMo_{0.5}$	BCC + σ phase	1.2659	53
$AlCo_{1.0}CrFeMo_{0.5}$	BCC + σ phase	1.2116	53
$AlCo_{1.5}CrFeMo_{0.5}$	BCC + σ phase	1.1681	53
$AlCo_{2.0}CrFeMo_{0.5}$	FCC + BCC + σ phase	1.1325	53
$AlCoFeNiMo_{0.5}$	BCC + σ phase	1.1171	54
$AlCoCr_{0.5}FeNiMo_{0.5}$	BCC + σ phase	1.1196	54
$AlCoCr_{1.0}FeNiMo_{0.5}$	BCC + σ phase	1.1216	54
$AlCoCr_{1.5}FeNiMo_{0.5}$	BCC + σ phase	1.1233	54
$AlCoCr_{2.0}FeNiMo_{0.5}$	BCC + σ phase	1.1248	54
$AlCoCrFeNiTi_{1.5}$	BCC + Laves phase	1.3539	6
$Al_{0.5}CoCrCuFeNi$	FCC	0.9198	34
$Al_{0.5}CoCrCuFeNiTi_{0.2}$	FCC	0.9672	34
$Al_{0.5}CoCrCuFeNiTi_{0.4}$	FCC + BCC1	1.0114	34
$Al_{0.5}CoCrCuFeNiTi_{0.6}$	FCC + BCC1 + BCC2	1.0527	34
$Al_{0.5}CoCrCuFeNiTi_{0.8}$	FCC + BCC1 + BCC2 + CoCr-like phase	1.0914	34

Table 1. *Cont.*

Alloys	Structure	$\overline{Md}$ (eV)	Refs
$Al_{0.5}CoCrCuFeNiTi_{1.0}$	FCC + BCC1 + BCC2 + CoCr-like phase	1.1277	34
$Al_{0.5}CoCrCuFeNiTi_{1.2}$	FCC + BCC1 + BCC2 + CoCr-like + Ti_2Ni-like phase	1.1618	34
$Al_{0.5}CoCrCuFeNiTi_{1.4}$	FCC + BCC1 + BCC2 + Ti_2Ni-like phase	1.194	34
$Al_{0.5}CoCrCuFeNiTi_{1.6}$	FCC + BCC1 + BCC2 + Ti_2Ni-like phase	1.2243	34
$Al_{0.5}CoCrCuFeNiTi_{1.8}$	FCC + BCC1 + BCC2 + Ti_2Ni-like phase	1.253	34
$Al_{0.5}CoCrCuFeNiTi_{2.0}$	FCC + BCC1 + BCC2 + Ti_2Ni-like phase	1.2801	34
$Al_{0.5}CoCrCuFeNiV_{0.2}$	FCC	0.9417	36
$Al_{0.5}CoCrCuFeNiV_{0.4}$	FCC + BCC	0.9621	36
$Al_{0.5}CoCrCuFeNiV_{0.6}$	FCC + BCC + σ phase	0.9811	36
$Al_{0.5}CoCrCuFeNiV_{0.8}$	FCC + BCC + σ phase	0.999	36
$Al_{0.5}CoCrCuFeNiV_{1.0}$	FCC + BCC + σ phase	1.0157	36
$Al_{0.5}CoCrCuFeNiV_{1.2}$	FCC + BCC	1.0314	36
$Al_{0.5}CoCrCuFeNiV_{1.4}$	FCC + BCC	1.0463	36
$Al_{0.5}CoCrCuFeNiV_{1.6}$	FCC + BCC	1.0603	36
$Al_{0.5}CoCrCuFeNiV_{1.8}$	FCC + BCC	1.0735	36
$Al_{0.5}CoCrCuFeNiV_{2.0}$	FCC + BCC	1.086	36
$AlCoCrFeNiMo_{0.1}$	BCC	1.088	37
$AlCoCrFeNiMo_{0.2}$	BCC + unidentified σ phase	1.0969	37
$AlCoCrFeNiMo_{0.3}$	BCC + unidentified σ phase	1.1055	37
$AlCoCrFeNiMo_{0.4}$	BCC + unidentified σ phase	1.1137	37
$AlCoCrFeNiMo_{0.5}$	BCC + unidentified σ phase	1.1216	37
$AlCoCrCuFeNiMo_{0.2}$	FCC + BCC	1.0192	38
$AlCoCrCuFeNiMo_{0.4}$	BCC + unidentified α phase	1.0358	38
$AlCoCrCuFeNiMo_{0.6}$	BCC + unidentified α phase	1.0514	38
$AlCoCrCuFeNiMo_{0.8}$	BCC + unidentified α phase	1.066	38
$AlCoCrCuFeNiMo_{1.0}$	BCC + unidentified α phase	1.0799	38
$AlCoCrFeNiNb_{0.1}$	BCC	1.0992	39
$AlCoCrFeNiNb_{0.25}$	BCC + (Laves phase + BCC)	1.1282	39
$AlCoCrFeNiNb_{0.5}$	BCC+ (Laves phase + BCC)	1.1732	39
$AlCoCrFeNiNb_{0.75}$	Laves phase + (Laves phase + BCC)	1.2142	39
CoCrFeNi	FCC	0.8735	42
$CoCrFeNiMo_{0.3}$	FCC	0.9207	42
$CoCrFeNiMo_{0.5}$	FCC + σ phase	0.9487	42
$CoCrFeNiMo_{0.85}$	FCC + σ+ + μ phase	0.9921	42
CoCrFeNi	FCC	0.8735	43
$CoCrFeNiTi_{0.3}$	FCC	0.971	43
$CoCrFeNiTi_{0.5}$	FCC + Laves + σ + R phase	1.0288	43
$Co_{1.5}CrFeNi_{1.5}Ti_{0.5}$	FCC	0.9775	55
$Co_{1.5}CrFeNi_{1.5}Ti_{0.5}Mo_{0.1}$	FCC	0.9878	55
$Co_{1.5}CrFeNi_{1.5}Ti_{0.5}Mo_{0.5}$	FCC + σ phase	1.0253	55
$Co_{1.5}CrFeNi_{1.5}Ti_{0.5}Mo_{0.8}$	FCC + σ phase	1.0502	55
$AlCoCrFeMo_{0.5}$	BCC + σ phase	1.2116	56
$AlCoCrFeMo_{0.5}Ni_{0.5}$	BCC + σ phase	1.1621	56
$AlCoCrFeMo_{0.5}Ni_{1.0}$	BCC + σ phase	1.1216	56

Table 1. *Cont.*

Alloys	Structure	$\overline{Md}$ (eV)	Refs
$AlCoCrFeMo_{0.5}Ni_{1.5}$	FCC+BCC + σ phase	1.0879	56
$AlCoCrFeMo_{0.5}Ni_{2.0}$	FCC+BCC + σ phase	1.0594	56
CoCrCuFeNi	FCC	0.8218	57
$CoCrCuFeNiTi_{0.5}$	FCC	0.9535	57
$CoCrCuFeNiTi_{0.8}$	FCC + Laves phase	1.0217	57
$CoCrCuFeNiTi_{1.0}$	FCC + Laves phase	1.0633	57
CoCrFeNiTi	FCC + BCC + Laves phase	1.153	58
$Al_{0.5}CoCrFeNiTi$	BCC1 + BCC2 + Laves phase	1.2209	58
$Al_{1.0}CoCrFeNiTi$	BCC1 + BCC2 + Laves phase	1.2775	58
$Ni_{0.2}Co_{0.6}Fe_{0.2}CrSi_{0.2}AlTi_{0.2}$	BCC + Cr_3Si	1.3698	59
$NiCo_{0.6}Fe_{0.2}CrSiAlTi_{0.2}$	BCC + Cr_3Si	1.3502	59
$NiCo_{0.6}Fe_{0.2}Cr_{1.5}SiAlTi_{0.2}$	BCC + Cr_3Si	1.3313	59
$CoFeNi_2V_{0.5}$	FCC	0.853	60
$CoFeNi_2V_{0.5}Nb_{0.2}$	FCC + Laves phase	0.907	60
$CoFeNi_2V_{0.5}Nb_{0.4}$	FCC + Laves phase	0.9566	60
$CoFeNi_2V_{0.5}Nb_{0.6}$	FCC + Laves phase	1.002	60
$CoFeNi_2V_{0.5}Nb_{0.65}$	FCC + Laves phase	1.0129	60
$CoFeNi_2V_{0.5}Nb_{0.7}$	FCC + Laves phase	1.0235	60
$CoFeNi_2V_{0.5}Nb_{0.75}$	FCC + Laves phase	1.0339	60
$CoFeNi_2V_{0.5}Nb_{0.8}$	FCC + Laves phase	1.0442	60
$CoFeNi_2V_{0.5}Nb$	FCC + Laves phase	1.0832	60
CoCrFeMnNbNi	FCC + Laves phase	1.095	61
CoCrCuFeNiNb	FCC + Laves phase	1.038	62
$Al_{0.5}CoCrNiTi_{0.5}$	FCC + BCC + B2 + σ phase	1.1804	63
$CoCrFeMo_{0.5}Ni$	FCC + σ phase	0.949	64
$Al_{0.5}CoCrFeMo_{0.5}Ni$	FCC + σ phase	1.0438	64
$AlCoCrFeMo_{0.5}Ni$	FCC + σ phase	1.1216	64
$Al_{1.5}CoCrFeMo_{0.5}Ni$	FCC + σ phase	1.1865	64
$Al_2CoCrFeMo_{0.5}Ni$	FCC + σ phase	1.2414	64
CoCrFeMnNi	FCC	0.8902	65
$CoCrFeMnNiV_{0.25}$	FCC	0.8823	65
$CoCrFeMnNiV_{0.5}$	FCC + σ phase	0.9495	65
$CoCrFeMnNiV_{0.75}$	FCC + σ phase	0.9753	65
CoCrFeMnNiV	FCC + σ phase	0.999	65

To further illustrate this point, the $\overline{Md}$ values for the HEA systems containing TCP phases were plotted in Figures 2 and 3, which clearly show the capability of $\overline{Md}$ to quantitatively predict the formation of TCP phases in HEAs. It was found that when $\overline{Md}$ > 1.09, stable TCP phases appeared except in a few exceptions where no TCP phases formed at $\overline{Md}$ < ~0.95. In the range of $\overline{Md}$ = ~0.95 to 1.09, the existence of TCP phases was unknown.

This is a novel method to predict the formation of TCP phases of HEAs. It must be pointed out that the theory may work well only in HEAs with high amounts of transition elements, especially, when these transition elements are Co, Cr, Cu, Fe, Ni, Mo, Ti, Mn, and Nb elements. It was found that the Laves

phase vanished in $Al_xCoCrFeNiTi_{0.5}$ alloys with high Al contents [66] and that the σ phase vanished in $Al_{0.5}CoCrCuFeNiV_x$ alloys with high V contents [36].

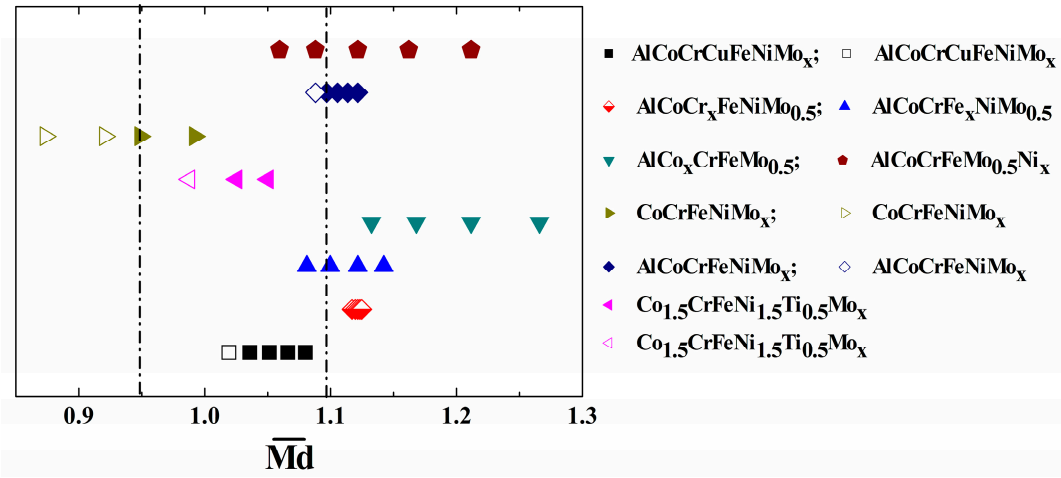

Figure 2. Relationship between the $\overline{Md}$ and the TCP phase stability for the HEA systems containing Al, Co, Cr, Fe, Ni, and Mo elements. Note on the legend: fully closed symbols and top-half closed symbols represent solid solution phase plus TCP phase; fully open symbols represent sole solid solution phases.

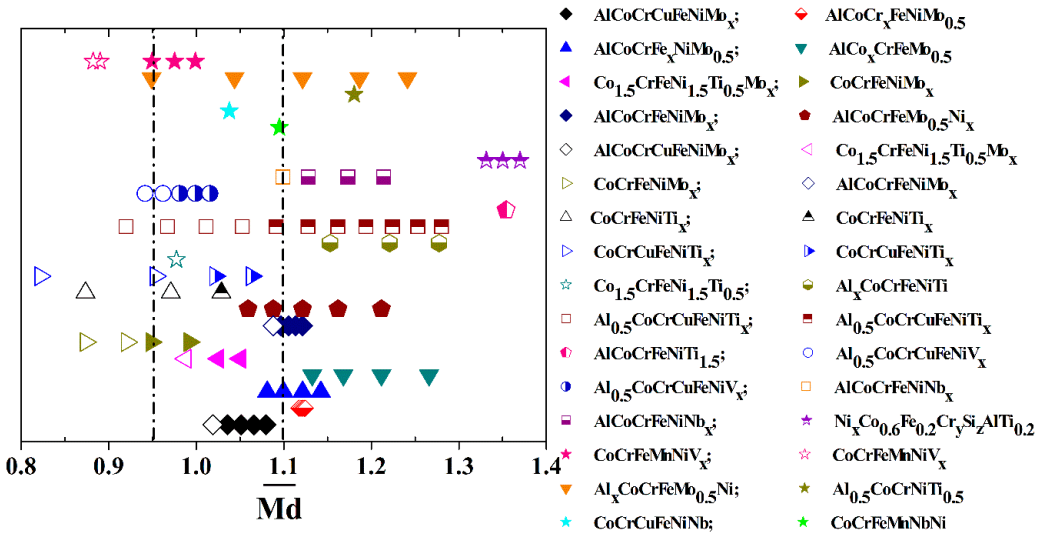

Figure 3. Relationship between the $\overline{Md}$ and the TCP phase stability for the HEA systems containing Al, Co, Cr, Cu, Fe, Ni, Mo, Si, Ti, V, Nb, and *etc.* elements. Note on the legend: fully closed symbols and top-half closed symbols represent solid solution phase plus TCP phase; fully open symbols represent sole solid solution phases.

This shows that the criterion $\overline{Md} > 1.09$ is invalid when the HEAs contain high levels of Al and V elements. The mechanisms of Al and V elements on the stability of TCP phases require further research. It should be noted that all statistic HEAs are nominal compositions in the paper. Therefore, in part of designed HEAs' composition there may be a deviation in the actual active content after melting. The target of this paper is to use some parameters to predict the phase formation in high-entropy alloys, and

from the prediction point of view only nominal compositions can be used, as actual compositions are only known after the materials are prepared. In this sense, the difference between the nominal composition and the actual composition is not a concern for the prediction we intend to make.

3. Conclusions

In this study, the average value of the energy level of the d-orbital ($\overline{Md}$) was used to predict the stability of TCP phases in HEAs. A TCP phase formation rule was proposed by calculating the $\overline{Md}$ value for HEAs containing Al, Co, Cr, Cu, Fe, Ni, Mo, Si, Ti, Nb and other transition elements. TCP phases were found to be stable at $\overline{Md} > 1.09$ except for some HEAs containing high levels of the elements Al and V. Specifically, it was discovered that the applicable alloying elements were limited to some transition elements (such as Co, Cr, Cu, Fe, Ni, Mn, Mo, Ti, and Nb), particularly as these elements easily formed the TCP phase. A novel method was used to predict the formation of TCP phases in HEAs. However, the significant impact of large amounts of Al and V elements on the stability of the TCP phase remains unclear, and therefore, more research is needed in order to fully understand it.

Acknowledgments

This work was supported by the National Natural Science Foundation of China Nos. (51104029, 51134013, and 51471044) respectively, the Fundamental Research Funds for the Central Universities, Key Laboratory of Basic Research Projects of Liaoning Province Department of Education (LZ2014007) and the Natural Science Foundation of Liaoning Province (2014028013). We would like to thank Prof. Zhijun Wang for helpful discussions.

Author Contributions

Yiping Lu and Yong Dong designed the research and wrote the paper. Li Jiang, Tingju Li and Tongmin Wang performed the data analysis. Yiping Lu, Tongmin Wang and Yong Zhang contributed to the results analysis and discussion. All authors have read and approved the final manuscript.

Conflicts of Interest

The authors declare no conflict of interest.

References

1. Cantor, B.; Chang, I.T.H.; Knight, P.; Vincent, A.J.B. Microstructural development in equiatomic multicomponent alloys. *Mater. Sci. Eng. A* **2004**, *375*, 213–218.
2. Yeh, J.W.; Chen, S.K.; Lin, S.J.; Gan, J.Y.; Chin, T.S.; Shun, T.T.; Tsau, C.H.; Chang, S.Y. Nanostructured high-entropy alloys with multiple principal elements: novel alloy design concepts and outcomes. *Adv. Eng. Mater*. **2004**, *6*, 299–303.
3. Zhang, Y.; Zuo, T.T.; Tang, Z.; Gao, M.C.; Dahmen, K.A.; Liaw, P.K.; Lu, Z.P. Microstructures and properties of high-entropy alloys. *Prog. Mater Sci.* **2014**, *61*, 1–93.
4. Chuang, M.-H.; Tsai, M.-H.; Wang, W.-R.; Lin, S.-J.; Yeh, J.-W. Microstructure and wear behavior of $Al_xCo_{1.5}CrFeNi_{1.5}$ Tiy high-entropy alloys. *Acta Mater.* **2011**, *59*, 6308–6317.

5. Hsu, C.Y.; Sheu, T.S.; Yeh, J.W.; Chen, S.K. Effect of iron content on wear behavior of AlCoCrFexMo$_{0.5}$Ni high-entropy alloys. *Wear* **2010**, *268*, 653–659.
6. Zhou, Y.J.; Zhang, Y.; Wang, Y.L.; Chen, G.L. Solid solution alloy of AlCoCrFeNiTi$_x$ with excellent room-temperature mechanical properties. *Appl. Phy. Lett.* **2007**, *90*, 181904.
7. Dong, Y.; Lu, Y.P.; Kong, J.R.; Zhang, J.J.; Li, T.J. Microstructure and mechanical properties of multi-component AlCrFeNiMo$_x$ high-entropy alloys *J. Alloys Compd.* **2013**, *573*, 96–101.
8. Senkov, O.N.; Scott, J.M.; Senkova, S.V.; Meisenkothen, F.; Miracle, D.B.; Woodward, C.F. Microstructure and elevated temperature properties of a refractory TaNbHfZrTi alloy. *J. Mater. Sci.* **2012**, *47*, 4062–4074.
9. Senkov, O.N.; Senkova, S.V.; Woodward, C.; Miracle, D.B. Low-density, refractory multi-principal element alloys of the Cr-Nb-Ti-V-Zr system: Microstructure and phase analysis. *Acta Mater.* **2013**, *61*, 1545–1557.
10. Chen, Y.Y.; Duval, T.; Hong, U.T.; Yeh, J.W.; Shih, H.C.; Wang, L.H.; Oung, J.C. Corrosion properties of a novel bulk Cu$_{0.5}$NiAlCoCrFeSi glassy alloy in 288 °C high-purity water. *Mater. Lett.* **2007**, *61*, 2692–2696.
11. Otto, F.; Yang, Y.; Bei, H.; George, E.P. Relative effects of enthalpy and entropy on the phase stability of equiatomic high-entropy alloys. *Acta Mater.* **2013**, *61*, 2628–2638.
12. Gludovatz, B.; Hohenwarter, A.; Catoor, D.; Chang, E.H.; George, E.P.; Ritchie, R.O. A fracture-resistant high-entropy alloy for cryogenic applications. *Science* **2014**, *345*, 1153–1158.
13. Hemphill, M.A.; Yuan, T.; Wang, G.Y.; Yeh, J.W.; Tsai, C.W.; Chuang, A.; Liaw, P.K. Fatigue behavior of Al$_{0.5}$CoCrCuFeNi high entropy alloys. *Acta Mater.* **2012**, *60*, 5723–5734.
14. Takeuchi, A.; Amiya, K.; Wada, T.; Yubuta, K.; Zhang, W.; Makino, A. Entropies in alloy design for high-entropy and bulk glassy alloys. *Entropy* **2013**, *15*, 3810–3821.
15. Koželj, P.; Vrtnik, S.; Jelen, A.; Jazbec, S.; Jagličić, Z.; Maiti, S.; Feuerbacher, M.; Steurer, W.; Dolinšek, J. Discovery of a superconducting high-entropy alloy. *Phys. Rev. Lett.* **2014**, *113*, 107001.
16. Senkov, O.N.; Wilks, G.B.; Miracle, D.B.; Chuang, C.P.; Liaw, P.K. Refractory high entropy alloys. *Intermetallics* **2010**, *18*, 1758–1765.
17. Lin, S.Y.; Chang, S.Y.; Chang, C.J.; Huang, Y.C. Nanomechanical properties and deformation behaviors of multi-component (AlCrTaTiZr)N$_x$Si$_y$ high-entropy coatings. *Entropy* **2014**, *16*, 405–417.
18. Lin, C.-M.; Tsai, H.-L.; Bor, H.-Y. Effect of aging treatment on microstructure and properties of high-entropy Cu$_{0.5}$CoCrFeNi alloy. *Intermetallics* **2010**, *18*, 1244–1250.
19. Lu, Y.P.; Dong, Y.; Guo, S.; Jiang, L.; Kang, H.J.; Wang, T.M.; Wen, B.; Wang, Z.J.; Jie, J.C.; Cao, Z.Q.; *et al.* A promising new class of high-temperature alloys: Eutectic high-entropy alloys. *Sci. Rep.* **2014**, *4*, doi: 10.1038/srep06200.
20. He, J.Y.; Liu, W.H.; Wang, H.; Wu, Y.; Liu, X.J.; Nieh, T.G.; Lu, Z.P. Effects of Al addition on structural evolution and tensile properties of the FeCoNiCrMn high-entropy alloy system. *Acta Mater.* **2014**, *62*, 105–113.
21. Guo, S.; Ng, C.; Lu, J.; Liu, C.T. Effect of valence electron concentration on stability of fcc or bcc phase in high entropy alloys. *J. Appl. Phys.* **2011**,*109*, 103505.
22. Raghavan, R.; Kumar, K.C.H.; Murty, B.S. Analysis of phase formation in multi-component alloys. *J. Alloy. Compd.* **2012,** *544*,152–158.

23. Singh, A.K.; Kumar, N.; Dwivedi A.; Subramaniam, A. A geometrical parameter for the formation of disordered solid solutions in multi-component alloys. *Intermetallics* **2014**, *53*, 112–119.
24. Tsai, K.Y.; Tsai, M.H.; Yeh, J.W. Sluggish diffusion in Co–Cr–Fe–Mn–Ni high-entropy alloys. *Acta Mater.* **2013**, *61*, 4887–4897.
25. Otto, F.; Dlouhy, A.; Somsen, C.; Bei, H.; Eggler, G.; George, E.P. The influences of temperature and microstructure on the tensile properties of a CoCrFeMnNi high-entropy alloy. *Acta Mater.* **2013**, *61*, 5743–5755.
26. Bhattacharjee, P.P.; Sathiaraj, G.D.; Zaid, M.; Gatti, J.R.; Lee, C.; Tsai, C.W.; Yeh, J.W. Microstructure and texture evolution during annealing of equiatomic CoCrFeMnNi high-entropy alloy. *J. Alloys Compd.* **2014**, *587*, 544–552.
27. Zhang, F.; Zhang, C.; Chen, S.L.; Zhu, J.; Cao, W.S. An understanding of high entropy alloys from phase diagram calculations. *Calphad* **2014**, *45*, 1–10.
28. Singh, A.K.; Subramaniam, A. On the formation of disordered solid solutions in multi-component. *J. Alloys Compd.* **2014**, *587*, 113–119.
29. Lee, C.P.; Chang, C.C.; Chen, Y.Y.; Yeh, J.W.; Shih, H.C. Effect of the aluminium content of $Al_xCrFe_{1.5}MnNi_{0.5}$ high-entropy alloys on the corrosion behaviour in aqueous environments. *Corros. Sci.* **2008**, *50*, 2053–2060.
30. Senkov, O.N.; Zhang, F.; Miller, J.D. Phase composition of a $CrMo_{0.5}NbTa_{0.5}TiZr$ high entropy alloy: Comparison of experimental and simulated data. *Entropy* **2013**, *15*, 3769–3809.
31. Gao, M.C.; Alman, D.E. Searching for next single-phase high-entropy alloy compositions. *Entropy* **2013**, *15*, 4504–4519.
32. Miracle, D.B.; Miller, J.D.; Senkov, O.N.; Woodward, C.; Uchic, M.D.; Tiley, J. exploration and development of high entropy alloys for structural applications. *Entropy* **2014**, *16*, 494–525.
33. Tsai, M.H.; Tsai, K.Y.; Tsai, C.W.; Lee, C.; Juan, C.C.; Yeh, J.W. Criterion for sigma phase formation in Cr- and V-containing high-entropy alloys. *Mater. Res. Lett.* **2013**, *1*, 207–212.
34. Chen, M.R.; Lin, S.J.; Yeh, J.W.; Chen, S.K.; Huang, Y.S.; Tu, C.P. Microstructure and properties of $Al_{0.5}CoCrCuFeNiTi_x$ (x = 0–2.0) high-entropy alloys. *Mater. Trans.* **2006**, *47*, 1395–1401.
35. Lee, C.P.; Chen, Y.Y.; Hsu, C.Y.; Yeh, J.W.; Shih, H.C. The effect of Boron on the corrosion resistance of the high entropy alloys $Al_{0.5}CoCrCuFeNiB_x$. *J. Electrochem. Soc.* **2007**, *154*, 424–430.
36. Chen, M.R.; Lin, S.J.; Yeh, J.W.; Chen, S.K.; Huang, Y.S.; Chuang, M.H. Effect of vanadium addition on the microstructure, hardness, and wear resistance of $Al_{0.5}CoCrCuFeNi$ high-entropy alloy. *Metall. Mater. Trans. A* **2006**, *37*, 1363–1369.
37. Zhu, J.M.; Fu, H.M.; Zhang, H.F.; Wang, A.M.; Li, H.; Hu, Z.Q. Microstructures and compressive properties of multicomponent $AlCoCrFeNiMo_x$ alloys. *Mater. Sci. Eng. A* **2010**, *527*, 6975–6979.
38. Zhu, J.M.; Zhang, H.F.; Fu, H.M.; Wang, A.M.; Li, H.; Hu, Z.Q. Microstructures and compressive properties of multicomponent $AlCoCrCuFeNiMo_x$ alloys. *J. Alloys Compd.* **2010**, *497*, 52–56.
39. Ma, S.G.; Zhang, Y. Effect of Nb addition on the microstructure and properties of AlCoCrFeNi high-entropy alloy. *Mater. Sci. Eng. A* **2012**, *532*, 480–486.
40. Zhu, J.M.; Fu, H.M.; Zhang, H.F.; Wang, A.M.; Li, H.; Hu Z.Q. Synthesis and properties of multiprincipal component $AlCoCrFeNiSi_x$ alloys. *Mater. Sci. Eng. A* **2010**, *527*, 7210–7214.

41. Zhou, Y.J.; Zhang, Y.; Kim, T.N.; Chen, G.L. Microstructure characterizations and strengthening mechanism of multi-principal component $AlCoCrFeNiTi_{0.5}$ solid solution alloy with excellent mechanical properties. *Mater. Lett.* **2008**, *62*, 2673–2676.
42. Shun, T.T.; Chang, L.Y.; Shiu, M.H. Microstructure and mechanical properties of multiprincipal component $CoCrFeNiMo_x$ alloys. *Mater. Charact.* **2012**, *70*, 63–67.
43. Shun, T.T.; Chang, L.Y.; Shiu, M.H. Microstructures and mechanical properties of multiprincipal component $CoCrFeNiTi_x$ alloys. *Mater. Sci. Eng. A* **2012**, *556*, 170–174.
44. Dong, Y.; Lu, Y.P.; Jiang, L.; Wang, T.M.; Li, T.J. Effects of electro-negativity on the stability of topologically close packed phase in high entropy alloys. *Intermetallic* **2014**, *52*, 105–109.
45. Ye, Y.F.; Wang, Q.; Lu, J.; Liu, C.T.; Yang, Y. The generalized thermodynamic rule for phase selection in multicomponent alloys. *Intermetallics* **2015**, *59*, 75–80.
46. Wang, Z.J.; Huang, Y.H.; Yang, Y.; Wang, J.C.; Liu, C.T. Atomic-size effect and solid solubility of multicomponent alloys. *Scr. Mater.* **2015**, *94*, 28–31.
47. Morinaga, M.; Yukawa, N.; Adachi, H. Superalloys. New PHACOMP and its application to alloy design. In Proceedings of the Fifth International Symposium Superalloys (1984), Seven Springs, PA, USA, 7–11 October 1984.
48. Morinaga, M.; Yukawa, N.; Adachi, H. Alloying effect on the electronic structure of Ni_3Al (γ'). *J. Phys. Soc. Jpn.* **1984**, *53*, 653–663.
49. Morinaga, M.; Yukawa, N.; Ezaki, H. Solid solubilities in transition-metal-based fcc alloys. *Phils. Mag. A* **1985**, *51*, 223–246.
50. Morinaga, M.; Yukawa, N.; Adachi, H. Alloying effect on the electronic structure of BCC Fe. *J. Phys. F* **1985**, *15*, 1071–1084.
51. Inoue, S.; Saito, J.; Morinaga, M.; Kano, S. Alloying effect on the electronic structures of Nb and Mo. *J. Phys. Condens. Matter.* **1994**, *6*, 5081–5096.
52. Pauling, L. *Nature of the Chemical Bond*; Cornell University press: Ithaca, NY, USA, 1960.
53. Hsu, C.Y.; Wang, W.R.; Tang, W.Y.; Chen, S.K.; Yeh, J.W. Microstructure and mechanical properties of new $AlCo_xCrFeMo_{0.5}Ni$ high-entropy alloys. *Adv. Eng. Mater.* **2010**, *12*, 44–49.
54. Hsu, C.Y.; Juan C.C.; Wang, W.R.; Sheu, T.S.; Yeh, J.W.; Chen S.K. On the superior hot hardness and softening resistance of $AlCoCrxFeMo_{0.5}Ni$ high entropy alloys. *Mater. Sci. Eng. A* **2011**, *528*, 3581–3588.
55. Chou, Y.L.; Yeh, J.W.; Shih, H.C. The effect of molybdenum on the corrosion behaviour of the high-entropy alloys $Co_{1.5}CrFeNi_{1.5}Ti_{0.5}Mo_x$ in aqueous environments. *Corros. Sci.* **2010**, *52*, 2571–2581.
56. Juan C.C.; Hsu, C.Y.; Tsai, C.W.; Wang, W.R.; Sheu, T.S.; Yeh, J.W.; Chen, S.K. On microstructure and mechanical performance of $AlCoCrFeMo_{0.5}Ni_x$ high-entropy alloys. *Intermetallics* **2013**, *32*, 401–407.
57. Wang, X.F.; Zhang, Y.; Qiao, Y.; Chen, G.L. Novel microstructure and properties of multicomponent $CoCrCuFeNiTi_x$ alloys. *Intermetallics* **2007**, *15*, 357–362.
58. Zhang, K.B.; Fu, Z.Y. Effects of annealing treatment on phase composition and microstructure of $CoCrFeNiTiAl_x$ high-entropy alloys. *Intermetallics* **2012**, *22*, 24–32.

59. Wang, L.M.; Chen, C.C.; Yeh, J.W.; Ke, S.T. The microstructure and strengthening mechanism of thermal spray coating $Ni_xCo_{0.6}Fe_{0.2}Cr_ySi_zAlTi_{0.2}$ high-entropy alloys. *Mater. Chem. Phys.* **2011**, *126*, 880–885.
60. Jiang, L.; Lu, Y.P.; Dong, Y.; Wang, T.M.; Cao, Z.Q.; Li, T.J. Effects of Nb addition on structural evolution and properties of the $CoFeNi_2V_{0.5}$ high-entropy alloy. *Appl. Phys. A* **2015**, *119*, 291–297.
61. Huo, W.Y.; Shi, H.F.; Ren, X.; Zhang, J.Y. Microstructure and wear behavior of CoCrFeMnNbNi high-entropy alloy coating by TIG cladding. *Adv. Mater. Sci. Eng.* **2015**, *2015*, doi: 10.1155/2015/647351.
62. Cheng, J.B.; Liu, D.; Liang, X.B.; Xu, B.S. Microstructure and electrochemical properties of CoCrCuFeNiNb high-entropy alloys coatings. *Acta. Metall. Sin.* **2014**, *27*, 1031–1037.
63. Lee, C.F.; Shun, T.T. Age hardening of the $Al_{0.5}CoCrNiTi_{0.5}$ high-entropy alloy. *Metall. Mater. Trans. A* **2014**, *45A*, 191–195.
64. Hsu, C.Y.; Juan, C.C.; Sheu, T.S.; Chen, S.K.; Yeh, J.W. Effect of aluminum content on microstructure and mechanical properties of $Al_xCoCrFeMo_{0.5}Ni$ high-entropy alloys. *JOM* **2013**, *65*, 1840–1847.
65. Stepanov, N.D.; Shaysultanov, D.G.; Salishchev, G.A.; Tikhonovsky, M.A.; Oleynik, E.E.; Tortika, A.S.; Senkov, O.N. Effect of V content on microstructure and mechanical properties of the $CoCrFeMnNiV_x$ high entropy alloys. *J. Alloys. Compd.* **2015**, *628*, 170–185.
66. Dong, Y.; Lu, Y.P.; Zhang, J.J.; Li, T.J. Microstructure and properties of multi-component $Al_xCoCrFeNiTi_{0.5}$ high-entropy alloys. *Mater. Sci. Forum.* **2013**, *745–746*, 775–780.